Nutrient supply to anticyclonic meso-scale eddies off western Australia estimated with artificial tracers released in a circulation model

H. Dietze [*],[1], R. Matear, T. Moore

Centre for Australian Weather and Climate Research (CAWCR), Hobart, Tasmania 7001, Australia[2]

ABSTRACT

The phytoplankton distribution off western Australia in the period from April to October is unique in that high biomass is generally associated with anticyclonic eddies and not with cyclonic eddies. As the western Australian region is oligotrophic this anomalous feature must be related to differing nutrient supply pathways to the surface mixed layer of cyclonic and anticyclonic eddies. A suite of modelled abiotic tracers suggests that cyclonic eddies are predominantly supplied by diapycnal processes that remain relatively weak until June–July, when they rapidly increase because of deepening surface mixed layers, which start to tap into the nutrient-replete waters below the euphotic zone. To the contrary, we find that anticyclonic eddies are predominantly supplied by injection of shelf waters, which carry elevated levels of inorganic nutrients and biomass. These injections start with the formation of the eddies in April–May, continue well into the austral winter and reach as far as several hundred kilometers offshore. The diapycnal supply of nutrients is suppressed in anticyclonic eddies since the injection of warm, low-salinity shelf waters delays the erosion of the density gradient at the base of the mixed layer. Our results are consistent with the observed seasonal cycles of chlorophyll *a* and observation of particulate organic matter export out of the surface mixed layer of an anticyclonic eddy in the region.

© 2009 Elsevier Ltd. All rights reserved.

1. Introduction

The region off western Australia (WA) is governed by the dynamics of the Leeuwin Current (LC), a poleward eastern boundary current. This control extends to the biogeochemistry in the region as, e.g. the geostrophic flows that support the LC suppress wind-driven upwelling of nutrient-replete water (Thompson, 1987). Further, it has been demonstrated that the current drives, via instability processes, meso-scale activity, which is correlated with ocean colour, primary production and nutrient uptake

(e.g. Waite et al., 2007b). This is most pronounced in austral autumn and winter when the LC increases its strength because of the weakening of opposing along-shore winds (Feng et al., 2003). The seasonality in surface chlorophyll is in phase with the current's strength. It is higher at the shelf break (where the LC is located) than offshore (Fig. 1) and puzzlingly, it is stronger in anticyclonic than in cyclonic features (Fig. 2). This is enigmatic since in the oligotrophic region off WA cyclonic eddies (CEs) are postulated to contain higher phytoplankton concentrations than anticyclonic eddies (ACEs). The explanation generally put forward for this is coined "eddy pumping": the formation and intensification of cyclonic eddies creates low sea level anomalies and upwelling of isopycnal surfaces at depth. This upwelling (eddy-pumping) can lift nutrient-replete waters into the euphotic zone, thereby fueling new production (e.g. Jenkins, 1988;

* Corresponding author.
E-mail address: hdietze@ifm-geomar.de (H. Dietze).
[1] Now at: IFM-GEOMAR, Leibniz Institute of Marine Sciences (at Kiel University), Kiel, Germany.
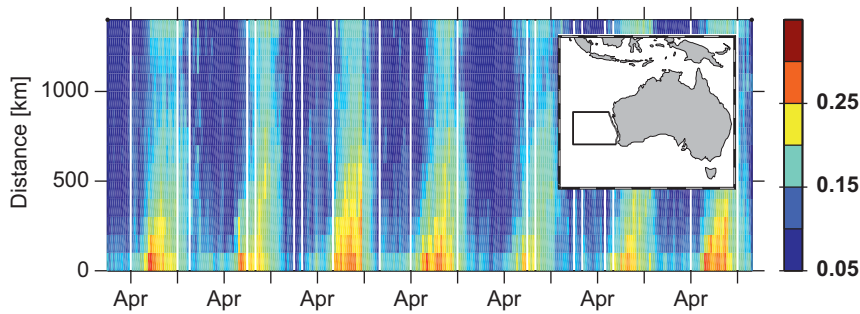[2] A partnership between CSIRO and the Bureau of Meteorology.

Fig. 1. Observed (SeaWiFS) chlorophyll *a* concentration for the period 1998–2004. The *y*-axis corresponds to distance from the shelf break (200 m isobath). Concentrations are averaged over the region bounded by 35–23°S and 100 km wide ribbons parallel to the shelf break. The unit is mg Chl a m^{-3}. The thick black line on the inlay map depicts the location of this study.
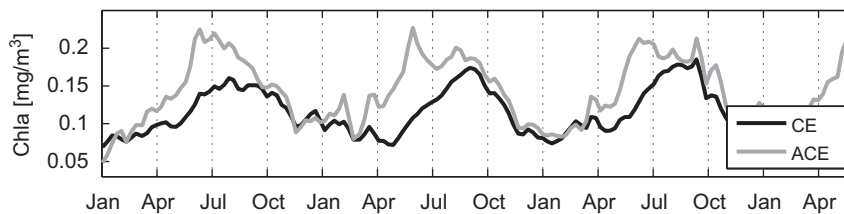

Fig. 2. Observed (SeaWiFS) chlorophyll concentration for the period 1998–2001. Concentrations are averaged over the region bounded by 100°E, the shelf break (here defined as the 200 m isobath) and 35–23°S (black line on the inlay map of Fig. 1). The black (grey) line refers to chlorophyll concentrations averaged over regions where sea surface (see Section 2.1) height is 0.2 m lower (higher) than the regional average.

Falkowski et al., 1991; McGillicuddy and Robinson, 1997). Subsequent turbulent vertical mixing, driven by the surface wind stress or negative surface buoyancy flux, might then transport phytoplankton (as well as nutrients) further up to the surface, where it can be observed by satellites. The formation (and intensification) of ACEs, on the other hand, is accompanied by downwelling fed by the convergence of horizontal (nutrient-depleted) surface currents, which deepen the surface mixed layer. This does not drive any transport of new nutrients to the euphotic zone (since it pushes the nutrient-depleted surface waters into the aphotic zone). In addition it reduces the average light level in the surface mixed layer (e.g. Tilburg et al., 2002). Hence, because of the differing physical frameworks, cyclonic eddies should be more productive and accommodate higher phytoplankton concentrations than their anticyclonic counterparts.

Feng et al. (2007) listed transport mechanisms potentially driving elevated (and anomalous) phytoplankton abundance in ACEs off WA, among them: (1) The eddy pumping argument applies only to the formation and growth of meso-scale eddies. During the decay of the eddies the sign of the effect reverses, i.e. the decay of ACEs (CEs) is associated with upwelling (downwelling) which might ultimately cause (no) nutrient supply to the surface mixed layer. (2) Instability processes or meso-scale eddy/wind interaction might be significant agents driving new production. (3) Coastal waters with high phytoplankton and particulate organic nitrogen (PON) concentrations might be preferentially exported into ACEs.

Here, we use a three-dimensional global circulation model, which is eddy resolving in the area of interest, to disentangle two pathways of nutrient supply to the surface mixed layer depth: nutrient supply from the shelf and supply from the thermocline below the euphotic zone. More specifically, we simulate various artificial tracers released on the shelf and in the thermocline to identify the origins of surface waters in ACEs. An artificial clock, counting the time elapsed since water parcels left the shelf, helps us to identify ACEs that have ceased to exchange water with the shelf.

2. Method

The main tool is a general ocean circulation model in an eddy-resolving configuration. Model results are combined with a nitrate climatology and remotely sensed chlorophyll *a* to quantify fluxes of "fixed nitrogen". We use sea surface height anomalies as observed from space to identify anticyclonic eddies in the observations.

2.1. Observations

The remotely sensed sea surface height anomalies (a blend of coastal tide gauges, European Space Agency Earth Resource Satellite and TOPEX/Poseidon altimeter data are described in Griffin et al., 2001). In the text, the CSIRO Atlas of Regional Seas is referred to as the CARS2000 climatology which is on a 0.5° × 0.5° grid on 56 vertical levels. The temporal resolution of the CARS2000 differs from most climatologies in that the time dependence at each grid box is given as amplitudes of annual sinusoids. The data and more related information are available at http://www.marine.csiro.au/~dunn/eez_data/atlas.html. SeaWiFS chlorophyll a data are level 3 mapped 8-day

composites obtained from http://seadas.gsfc.nasa.gov/ftp.html.

2.2. Numerical model

We embedded (online) various tracers into a global configuration of the MOM4p0d (GFDL Modular Ocean Model v.4, Griffies et al., 2005) ocean circulation model. The horizontal resolution is $2°$ telescoping to $\frac{1}{10}°$ within $90°E$ to $180°E$ and $75°S$ to $16°N$. The vertical grid has a total of 47 levels, 25 of these within the upper 300 m. Configuration and initialization are identical to those in the spinup of the Ocean Forecasting Australia Model (OFAM) without data assimilation, described by Oke et al. (2005): the atmospheric forcing consists of diurnal wind stress, heat and freshwater fluxes as derived from the years 1992 to 2002 of the ERA-40 re-analyses of Uppala et al. (2005). A flux correction restores sea surface temperatures (SST) with a timescale of 30 days to monthly mean SST derived from a blend of satellite products (Rathbone, 2006, personal communications). The circulation model was spun up by integrating over the 1994–2002 period two times. The results presented here refer to a third run through the period. The tracer releases start in 1996. The evolution of the passive tracers is determined by an advective–diffusive equation identical to that of temperature and salinity. The numerical implementation of tracer (and momentum) advection is based on the third-order upwind-biased flux limited approach of Hundsorfer and Trompert (1994), which is the default setting in MOM4p0d. The vertical mixing of momentum and passive tracers is parameterized following Chen et al. (1994): in the surface mixed layer a modified Kraus–Turner-type mixed layer model accounts for the mixing of tracers. Viscosity is parameterized as a function of the local Richardson number throughout the water column. The same applies for diffusivities below the surface mixed layer. Minimum values for viscosity and diffusivity, accounting for turbulence induced by the internal wave field, are set to 2×10^{-5} and $1 \times 10^{-6}\,m^2\,s^{-1}$, respectively. Actual diapycnal mixing will, however, exceed these explicit values since the numerical advection scheme introduces additional numerically induced, spurious mixing, which is difficult to estimate (e.g. Burchard and Rennau, 2008).

(1) To quantify the relative contribution of shelf water in % that was in contact with the Australian shelf a tracer was initialized with 0% in every grid box and continuously reset to 100% on the Australian shelf (here defined as the 200 m isobath, e.g. Fig. 3). The release started on 1st January 1996 and ran for 1 year. A second tracer, a primitive age tracer, was also initialized with zero in every grid box on 1st January 1996 but counted up time in every grid box, except on the Australian shelf, where age was continuously reset to zero. Thus, this age tracer gives an estimate of the time elapsed, since a water parcel was in contact with the Australian shelf.

(2) To quantify the relative contribution of thermocline waters entering the surface mixed layer 4 tracers were initialized with 0% above and 100% below specific depth levels (Z_r). The depth levels Z_r were 125, 135, 175 and 195 m. These tracer releases started on 1st May 1996. (The late start was chosen as a compromise between covering the period of surface mixed layer deepening in the region and saving computation time.) Fig. 4 panel (A) shows the distribution of the $Z_r = 125$ m tracer along a vertical section one day after its release. After initialization neither sources nor sinks were added. In the following section we combine concentrations of these tracers in the surface mixed layer with climatological nitrate concentrations in the thermocline to calculate the associated nitrate supply. More specifically, the difference of the surface mixed layer concentrations of two thermocline tracers released at two subsequent depth levels Z_r is an estimate of how much of the surface mixed layer water originates from the depth
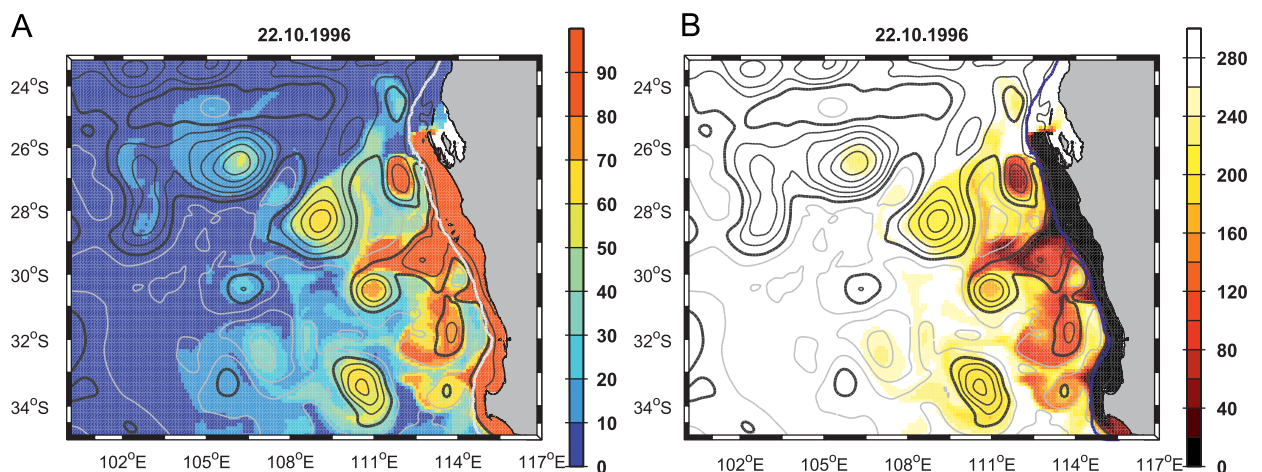

Fig. 3. Snapshot of modelled surface concentrations of artificial tracers in October. Dark and lighter grey contours denote positive and negative sea surface height anomalies, respectively. Contour intervals are 10 cm. The shelf break is marked with a white and a blue line in panels (A) and (B), respectively. Panel (A): The colour denotes "shelf water" content in % as in Fig. 8. The colour shading in panel (B) indicates the time elapsed since the surface water was in contact with the Australian shelf. The unit is days. (For interpretation of the reference to colour in this figure legend, the reader is referred to the web version of this article.)
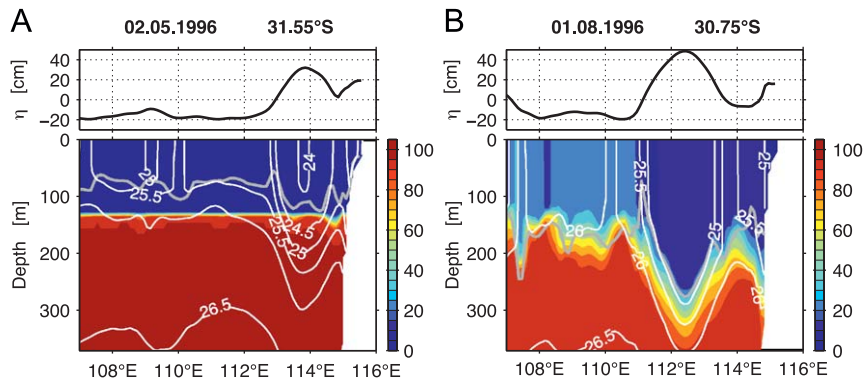
Fig. 4. Zonal sections through the centre of a modelled anticyclonic eddy (ACE). Panels (A) and (B) refer to daily averages at times indicated in the respective titles. Note that this eddy is marked with a black cross in Fig. 8. The upper panels refer to sea surface height anomalies (η). White contours in the lower panels are densities σ_0, the grey lines are the surface mixed layer depths (here defined as the depth where σ_0 is 0.125 higher than at the surface) while the colour shadings refer to the "thermocline water" content in % which is used to quantify diapycnal transport processes (such as vertical entrainment) supplying deep (high nutrient) water to the surface mixed layer of a growing and deepening eddy. The "thermocline water" tracers are initialized with zero above a specific depth level Z_r on the 1st May 1996. Below Z_r the tracers are initialized with 100%. Note that there is no restoring, neither at the surface nor at depth. This figure refers to the experiment with $Z_r = 125$ m. (For interpretation of the reference to colour in this figure legend, the reader is referred to the web version of this article.)

interval bounded by the two depth levels. Multiplication of this estimate with the nitrate concentration representative for the respective depth interval yields that fraction of the "fixed nitrogen" concentration in the surface mixed layer that is introduced by water originating from the depth interval bounded by the two depth levels Z_r.

The nitrate concentrations are extracted from the CARS2000 (Section 2.1) climatology. Nitrate fluxes are calculated by averaging, each model day, nitrate data comprised by respective depth levels Z_r and a $2° \times 2°$ square centred around the model grid boxes. This average nitrate concentration is multiplied with respective daily increases in thermocline water concentration found in the surface mixed layer. For the deepest tracer release $Z_r = 195$ m we calculate the associated nitrate concentration as the mean over the 195–250 m depth interval.

3. Results

The modelled southward flowing Leeuwin current shows, in agreement with observations (not shown), high seasonal variability with increased southward flow starting in April when the prevailing southerly winds weaken. The peak flow is in June, and high flow continues into October (see sea surface height anomaly contours in Fig. 3, panel (A)). The increased flow fuels instabilities and, consequently, large meanders evolve along the shelf-break boundary between the coastal waters off the central WA shelf and those offshore. These meanders grow and eventually become free ACEs, which drift northwestwards with a lifespan of about a year. Maximal surface mixed layer depths reached during austral winter/spring are between 250 and 300 m in modelled ACEs, agreeing well with the only observations we are aware of (250 m by Moore et al., 2007 and 285 m by Feng et al., 2007). The following section describes differing pathways of nutrient supply to cyclonic and anticyclonic features averaged over the region bounded by 100°E, the shelf break (here defined as the 200 m isobath) and 35–23°S (depicted as

black line in the inlay map of Fig. 1). In Section 3.2 we focus on nutrient supply to a typical modelled ACE.

3.1. Differing nutrient supply pathways to the surface mixed layer depth of cyclonic and anticyclonic features

Satellite observations show a pronounced seasonal cycle in surface chlorophyll concentrations which increases towards the shelf break (Fig. 1). They further reveal that the cycle is more pronounced in ACEs than in CEs as average surface chlorophyll concentrations in ACEs exceed those found in CEs during the April until October period (Fig. 2). Snapshots of sea surface height anomalies and ocean colour (Fig. 5) suggest that this is related to a preferential input of shelf waters carrying high chlorophyll levels to anticyclonic eddies. To test this idea an artificial (model) tracer was continuously released on the shelf (Section 2.2). The tracer tags water parcels originating from the shelf, which we will call "shelf water". Fig. 6 panel (A) partitions the total volume of "shelf water" found offshore of the 200 m isobath into that fraction found in anticyclonic and cyclonic features (here defined as areas with sea surface height anomalies higher and lower than zero), respectively. We conclude that "shelf water" is preferentially exported into anticyclonic features until the beginning of July.

An additional source of nutrient to the surface mixed layer is diapycnal mixing, which transports thermocline waters high in nutrients to the nutrient-depleted surface. To that end, convection, driven by buoyancy losses at the surface and associated with entrainment of thermocline waters into a deepening surface mixed layer, is generally a major process. Fig. 7 shows modelled, spatially averaged surface mixed layer depths for cyclonic and anticyclonic features. On average, the surface mixed layer deepens faster in cyclonic than in anticyclonic features during austral autumn and winter. Moreover, it peaks at values exceeding the depth of the euphotic zone by around 75 m, whereas in anticyclonic features the euphotic zone is only
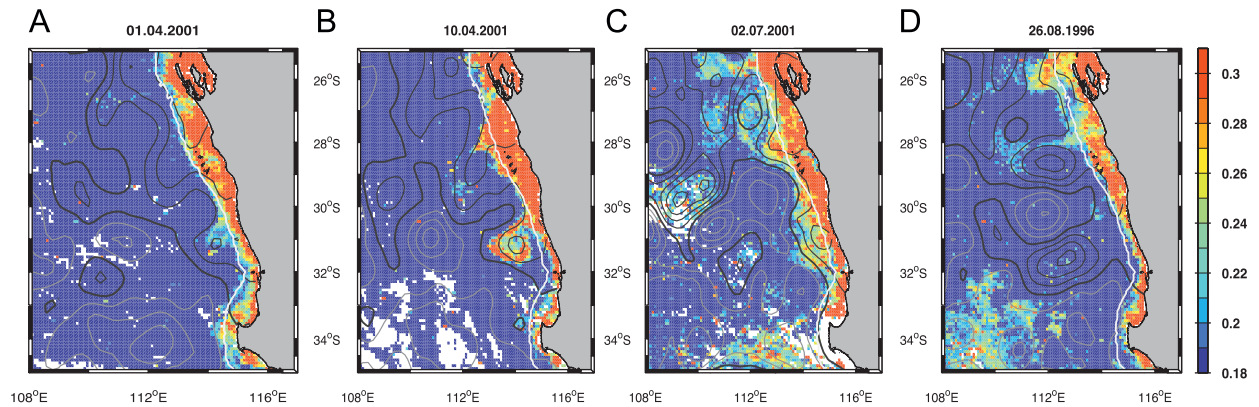
Fig. 5. Observed evolution of chlorophyll and sea surface height anomalies off western Australia. Colour shading is in units mg Chl$a$ m^{-3} from SeaWiFS, values below 0.18 and above 0.3 are capped. White pixels represent missing data. The white line denotes the 200 m isobath from ETOPO5 (National Geophysical Data Centre, NGDC, 1988). The thick black line is the 0 m sea surface height anomaly isoline. Thinner grey (black) lines denote negative (positive) sea surface height anomalies. The contour interval is 0.1 m. Note that panel (D) refers to the year 2003 since the respective 2001 snapshot is obscured by clouds. (For interpretation of the reference to colour in this figure legend, the reader is referred to the web version of this article.)
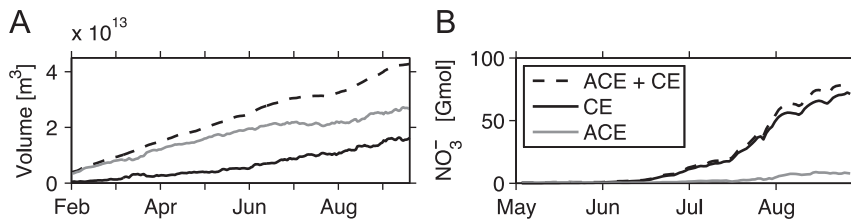

Fig. 6. Modelled nutrient supply pathways integrated over the region bounded by 100°E, the shelf break (200 m isobath) and 35–23°S (dashed line). The black (grey) line refers to the integral over all regions where sea surface height is lower (higher) than the regional average. Panel (A) refers to the volume of water stemming from the shelf (i.e. onshore of the 200 m isobath). Panel (B) shows the total nitrate entrained from the thermocline to the surface mixed layer depth (here defined as in Fig. 4).
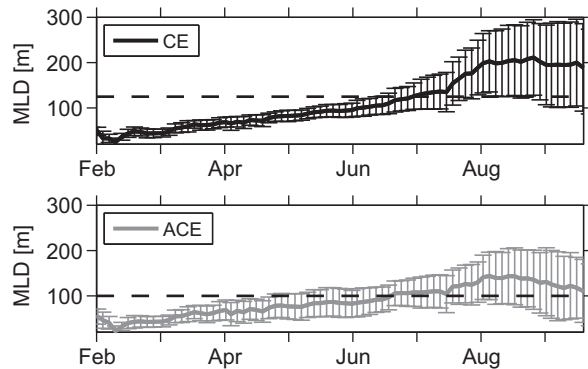

Fig. 7. Modelled surface mixed layer depths (MLDs, defined as in Fig. 4). MLDs are averaged over the region bounded by 100°E, the shelf break (200 m isobath) and 35–23°S. Error bars denote standard deviations from the regional mean. Upper (lower) panel refers to all surface mixed layer depths where the modelled sea surface height anomalies were less (greater) than zero. The dashed black lines in both panels denote the respective depths of the euphotic zone derived from ocean colour by Moore et al. (2007).

exceeded by 50 m in austral winter. Hence, since cyclonic features tap deeper into the nutrient-replete waters below the euphotic zone, the entrainment of nutrients due to surface mixed layer deepening should be more significant in cyclonic features. The reason for that can be related

back to the fact that in the region, anticyclonic eddies generally have higher sea surface temperatures, corresponding to higher heat contents in the surface mixed layers, which delays the erosion of the density gradient at the base of the mixed layer.

Fig. 6 panel (B) shows a model estimate of diapycnal nitrate supply to the surface mixed layer for both cyclonic and anticyclonic features. By model formulation this includes (1) mixing induced by surface mixed layer deepening driven by buoyancy losses at the surface, (2) mixing associated with Kelvin–Helmholtz instabilities and (3) the effect of internal waves fueling turbulence in the interior. The latter parameterization is rather on the low end of mixing rates observed elsewhere (Section 2.2). Further, the effect of double diffusive fluxes, which was shown to be significant in subtropical regions elsewhere (e.g. Dietze et al., 2004), was neglected. But then, on the other hand, the magnitude of diapycnal numerical mixing might well exceed realistic levels (e.g. Burchard and Rennau, 2008). We conclude that the estimates presented here are uncertain, and a thorough evaluation of modelled diapycnal fluxes has to await turbulence measurements in the region. The relative importance of diapycnal nutrient supply to cyclonic and anticyclonic features, however, should be relatively robust since, to first order, both regimes will be affected in a similar way by model deficiencies.

Fig. 6 is based on a set of artificial tracers released in the model. These tracers quantify the amount of nutrient-replete waters originating from below the euphotic zone (apparently at 100 and 125 m depth for ACEs and CEs, respectively, as Moore et al., 2007 conclude based on the 1% level of photosynthetically active radiation relative to the surface) that enter the surface mixed layer depth. Fig. 6 reveals that the nitrate supply integrated over the beginning of May until end of August period and the region bounded by 100°E, the shelf break (here defined as the 200 m isobath) and 35–23°S is 71 and 8 Gmol NO_3^- for cyclonic and anticyclonic features, respectively. This corresponds to 208 and 33 mmol NO_3^- m^{-2} year^{-1} and implies that diapycnal mixing processes are contributing almost an order of magnitude less nitrate to the surface mixed layer of anticyclonic features than to the surface mixed layer of cyclonic features. The highest fluxes occur during July where the surface mixed layer deepens rapidly beyond the depth of the euphotic zone. This is strong evidence that convection is indeed the major process driving diapycnal fluxes to the surface mixed layer.

3.2. Chronology of "fixed nitrogen" supply to a typical anticyclonic meso-scale eddy

By tracking a typical modelled ACE through time the "shelf water" tracer experiment reveals that shelf waters are intermittently injected into the rim of the ACE starting with the formation of the meander and continuing for months, well into austral winter, as far as several hundred kilometers offshore (Figs. 8 and 9, panel (A)). This transport mechanism is so efficient that more than 50% of the water encompassed by the eddies' surface mixed layer stems from the shelf at any given time (Fig. 8), while typical concentrations are more than 60 ± 10%. This holds even though the volume comprised by the ACE's surface mixed layer increases by more than 400% (Fig. 9, panel (B)) because of converging surface currents driving an increase in the horizontal extent of the eddy and (in combination with sea-air heat fluxes) a threefold increase in the surface mixed layer depth during the growth phase

of the eddy from April until the end of July (Fig. 9, panel (A)).

Zonal sections through the ACE in May and August (Fig. 4) reveal that the density in the surface mixed layer increased while the deepening took place. This is a clear indication that diapycnal transport of thermocline waters to the surface mixed layer must have occurred. We use a set of tracers released at various depths below the euphotic zone to quantify this diapycnal contribution. Fig. 4 panel (A) shows a zonal section through the ACE corresponding to a time before the mixed layer starts deepening monotonically for a tracer released below 125 m. From the surface down to 125 m the tracer
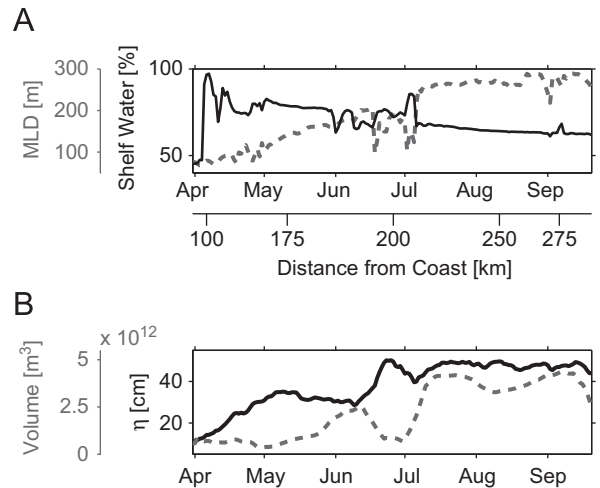

Fig. 9. Temporal evolution of properties at the centre of the modelled anticyclonic eddy which is marked by a black cross in Fig. 8. The centre of the eddy is defined as the local maximum of sea surface height. Panel (A), dashed grey line denotes the surface mixed layer depth (MLD, defined as in Fig. 4); the black line refers to the shelf water content in the MLD. Panel (B), black line denotes the sea surface height anomaly (η). The dashed grey line refers to the volume encompassed by the surface mixed layer of the anticyclonic eddy (here defined as all waters in the vicinity of the anticyclonic eddie's centre which have densities σ_0 less than 0.125 kg m^{-3} apart from the density in the MLD of the eddy centre).
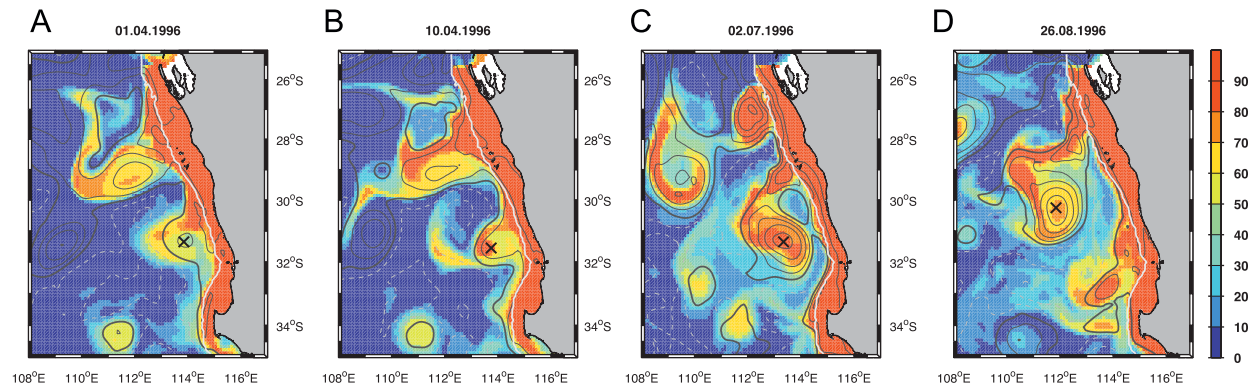

Fig. 8. Modelled surface concentrations of an artificial tracer continuously released on the shelf. Colour shading is that fraction of water that came from the Australian shelf after 1st January 1996. The units are %. 100% corresponds to water parcels that are entirely from the shelf. Dark grey and lighter grey lines contour positive and negative sea surface height anomalies, respectively. The contour interval is 10 cm. The black cross marks the centre of the ACE, which is examined further in Figs. 9 and 10. (For interpretation of the reference to colour in this figure legend, the reader is referred to the web version of this article.)
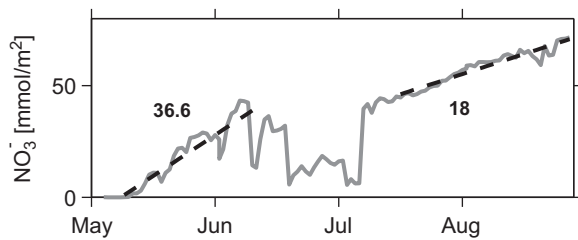
Fig. 10. Modelled temporal evolution of that fraction of NO_3^- in the surface mixed layer that is caused by import of thermocline water. This evolution refers to concentrations in the centre of the anticyclonic eddy, which is marked by a black cross in Fig. 8. The black numbers 36.6 and 18 mmol NO_3^- m^{-2} month^{-1} refer to the slopes calculated over the periods that are indicated by the dotted black lines.

concentration is zero, indicating that no thermocline water has crossed the 125 m depth level since the initialization of the tracer. At the end of August (Fig. 4, panel (B)), after the mixed layer deepening, the tracer concentration reached 17.5, revealing that 17.5% of the water encompassed by the ACEs' surface mixed layer stems from thermocline waters that were below 125 m at 1st May. By subtracting "thermocline water" concentrations, as modelled by releasing the "thermocline tracers" below different depths, the origin of entrained waters can be broken down into greater detail and associated nitrate concentrations can be assigned as described in Section 2.2. We find a diapycnal supply of nitrate to the surface layer of the ACE of 78 mmol m^{-2} over the 4-month period from 1st May to 31st August. The diapycnal supply is not constant in time (Fig. 10): it does not rise to significant levels until the beginning of May, when the deepening surface mixed layer depth starts to tap into nutrient-replete waters below the euphotic zone at ≈ 100 m (Fig. 9, panel (A)). It stays at a fairly constant 37 mmol NO_3^- m^{-2} month^{-1} until it stalls in June until the beginning of July. During that period the eddy undergoes a remarkable change: the sea surface height anomaly increases rapidly (Fig. 9, panel (B)), and shelf water is entrained intermittently as can be derived from the undulating shelf water concentrations (Fig. 9, panel (A)). The shelf water is warmer and lighter and enters the eddy predominantly at the surface, which results in temporary vertical density gradients within the formerly homogenous surface mixed layer. Subsequent mixing erodes the gradients and drives an oscillating surface mixed layer depth (which is defined using a density criterion). The volume of the eddy apparently declines (Fig. 9, panel (B)), but this is an artefact of the definition, which is based on a density criterion. Overall, the emerging picture for the period from June until the beginning of July is a rapid growth of the ACE, which is mainly fueled by converging surface currents stemming from the shelf. These currents increase the sea surface height anomaly and push the base of the surface mixed layer depth down to 285 m. This deepening of the surface mixed layer differs from convection as it is not associated with entrainment of thermocline waters. Fig. 4 highlights this process: in May (panel (A)) the surface mixed layer depth of the ACE is just slightly above the thermocline tracer, which was released one day earlier. The density

within the surface mixed layer is around $\sigma_0 = 24$. In August (panel (B)) the surface mixed layer depth has deepened down to 285 m and the density therein has reached $\sigma_0 = 25$. As, in August, thermocline tracer concentrations are still relatively low, most of the surface mixed layer deepening must have been driven by converging surface currents, rather than by (diapycnal) entrainment.

In the second half of July disturbances by shelf water are weak and rare (Fig. 9, panel (A)), the water encompassed by the eddy is relatively homogenous and the diapycnal supply of nitrate recurs at a fairly constant 18 mmol m^{-2} month^{-1} (Fig. 10) until the end of the experiment. During that phase, modelled ACEs are surprisingly stable: Fig. 3 panel (B) shows a snapshot from the end of October of the time elapsed since surface waters were in contact with the shelf. In combination with Fig. 3 panel (A) this reveals that ACEs isolated from the coastal waters for more than half a year still have a "shelf water" content of more than 50%. We conclude that, on timescales of several months, the horizontal exchange of water across the boundaries of fully grown ACEs as well as the associated loss of "fixed nitrogen" is not of leading order.

4. Discussion

Qualitatively, satellite data confirms that shelf waters with high chlorophyll concentrations are predominantly exported into ACEs (Fig. 5). Moreover, the differing observed seasonal cycles of chlorophyll in ACEs and CEs are consistent with our findings: in ACEs phytoplankton concentrations rise rapidly from January until June–July, which coincides with the period where shelf water, carrying elevated phytoplankton concentrations, is predominantly exported into ACEs. The increase in phytoplankton concentrations in CEs, on the other hand, reaches a maximum around July, when vertical entrainment associated with deepening surface mixed layers start to tap into the nutrient-replete waters below the euphotic zone. The maximum of phytoplankton concentrations in CEs is reached in August–September, when the surface mixed layers approach their annual maxima.

A crucial question remains whether our estimates of "fixed nitrogen" supply to the surface mixed layer depth of ACEs balance losses and changes in standing stocks, i.e. whether they are sufficient to close the budget. The model results presented in the previous section showed that physical transport mechanisms exchanging water across the eddies boundary are not a significant loss term to the "fixed nitrogen" encompassed in the surface mixed layer of the ACE. This occurs in the model even though numerical advection schemes similar to the one used here have been shown to introduce large levels of spurious, numerically induced, mixing (Burchard and Rennau, 2008). Hence, most likely, our model estimate of (small) cross-eddy mixing is biased high and suggests that export of particulate organic nitrogen sinking out of the surface mixed layer is the main loss term. Problematic in that respect is that there is only one direct

measurement of export out of an ACE to compare our results with: in October 2003 Greenwood et al. (2007) measured an export of $42\,\text{mmol}\,\text{N}\,\text{m}^{-2}\,\text{month}^{-1}$ with a sediment trap deployed below the surface mixed layer, which extended down to 285 m. (Note that the associated error is highly uncertain since sediment trap data are notoriously difficult to interpret because of issues such as trapping efficiency, swimmers migrating into the trap and dissolution of trapped particulate organic matter.) In the same eddy, surface nitrate was depleted down to detection limit and the PON to chlorophyll a ratio was $2.05 \pm 0.63\,\text{mmol}\,\text{N}\,(\text{mg Chl}a)^{-1}$ (Waite et al., 2007a). Typical rates of chlorophyll a decline in ACEs in October are $30 \pm 10\,\mu\text{g}\,\text{Chl}a\,\text{m}^{-3}\,\text{month}^{-1}$ (obtained by linear fits to Fig. 2), which yields a corresponding decline in PON of

$$2.05\,\text{mmol}\,\text{N}\,(\text{mg Chl}a)^{-1} \times 30\,\mu\text{g}\,\text{Chl}a\,\text{m}^{-3}\,\text{month}^{-1}$$
$$\times\,285\,\text{m} = 18 \pm 8\,\text{mmol}\,\text{N}\,\text{m}^{-2}\,\text{month}^{-1} \qquad (1)$$

for a 285 m deep surface mixed layer. So we conclude that a sum of PON export and changes in standing stocks within the surface mixed layer of $24 \pm 8\,\text{mmol}\,\text{N}\,\text{m}^{-2}\,\text{month}^{-1}$ must be balanced by supply of "fixed nitrogen". Note that the actual error is much higher as we did not account for (unknown) uncertainties of the sediment trap estimate. The ACE described in Greenwood et al. (2007) and Waite et al. (2007a) was relatively stable in terms of sea surface height anomaly and horizontal extent (Feng et al., 2007, Fig. 7) and as a visual inspection of SeaWiFS ocean colour did not show any recent apparent entrainment of water stemming from the shelf we conclude that the characteristics of the observed ACE match those of our modelled (and closely examined) one during August. For this period the combination of the thermocline tracer release experiment with climatological nitrate concentrations yielded diapycnal supply of $18\,\text{mmol}\,\text{NO}_3^-\,\text{m}^{-2}\,\text{month}^{-1}$ (Fig. 10) which is consistent with the $24 \pm 8\,\text{mmol}\,\text{N}\,\text{m}^{-2}\,\text{month}^{-1}$ anticipated above.

The calculation of a "fixed nitrogen" budget in ACEs comprising their growth phase is, naturally, even more uncertain, since the above-mentioned measurements of export and PON to chlorophyll ratio have to be extrapolated in time. It remains to show if such an approach is admissible. Nevertheless we present a rough calculation for the period from 1st April until 1st October: within that period, chlorophyll a concentrations in ACEs typically rise by $17\,\mu\text{g}\,\text{Chl}a\,\text{m}^{-3}$ (Fig. 2). Based on the PON to chlorophyll ratio used above and a surface mixed layer depth of 285 m this corresponds to an increase of

$$2.05\,\text{mmol}\,\text{N}\,(\text{mg Chl}a)^{-1} \times 17\,\mu\text{g}\,\text{Chl}a\,\text{m}^{-3} \times 285\,\text{m}$$
$$= 7\,\text{mmol}\,\text{N}\,\text{m}^{-2}. \qquad (2)$$

Extrapolation of the export measurement yields a loss of

$$7\,\text{months} \times 42\,\text{mmol}\,\text{N}\,\text{m}^{-2}\,\text{month}^{-1} = 294\,\text{mmol}\,\text{N}\,\text{m}^{-2}. \qquad (3)$$

Hence, in total, approximately $300\,\text{mmol}\,\text{N}\,\text{m}^{-2}$ must be supplied to the surface mixed layer of an ACEs from 1st April to 1st October.

Typically ACEs have a shelf water content of $60 \pm 10\%$ half a year after they were spun off the shelf as the combination of the "shelf tracer" and the age tracer in Fig. 3 reveals. Based on typical nitrate ($0.3 \pm 0.1\,\text{mmol}\,\text{NO}_3^-\,\text{m}^{-3}$) and chlorophyll concentrations ($0.6 \pm 0.2\,\text{mg}\,\text{Chl}a\,\text{m}^{-3}$) observed on the shelf (Lourey et al., 2006) during the April until July period when, according to our results, strong shelf water injection (Fig. 6, panel (A)) coincides with increasing chlorophyll concentrations in ACEs (Fig. 2), we calculate the supply of "fixed nitrogen" from the shelf as: $285\,\text{m} \times 60\% \times (0.3\,\text{mmol}\,\text{NO}_3^-\,\text{m}^{-3} + 0.6\,\text{mg}\,\text{Chl}a\,\text{m}^{-3} \times 2.05\,\text{mmol}\,\text{N}\,(\text{mg Chl}a)^{-1}) = 260\,\text{mmol}\,\text{N}\,\text{m}^{-2}$. In addition, Fig. 10 suggests that diapycnal supply of nitrate does not rise to significant levels until May ($37\,\text{mmol}\,\text{NO}_3^-\,\text{m}^{-2}\,\text{month}^{-1}$), when the surface mixed layer depth reaches the euphotic zone; it is stalled around June when supply of warm shelf water suppresses convection and recurs in July at a rate of $18\,\text{mmol}\,\text{NO}_3^-\,\text{m}^{-2}\,\text{month}^{-1}$, staying constant until the end of the experiment in September. We speculate that the $18\,\text{mmol}\,\text{NO}_3^-\,\text{m}^{-2}\,\text{month}^{-1}$ is representative throughout September (although our experiments end at the beginning of September) and calculate the nitrate supply due to diapycnal processes from 1st April until 1st October as $1\,\text{month} \times 37\,\text{mmol}\,\text{NO}_3^-\,\text{m}^{-2}\,\text{month}^{-1} + 3\,\text{month} \times 18\,\text{mmol}\,\text{NO}_3^-\,\text{m}^{-2}\,\text{month}^{-1} = 90\,\text{mmol}\,\text{NO}_3^-\,\text{m}^{-2}$. Hence, in total we find a supply of $350 \pm 100\,\text{mmol}\,\text{NO}_3^-\,\text{m}^{-2}$ to a typical ACE for the 1st April until 1st October which is consistent with observed changes in standing stocks and an, admittedly highly uncertain, estimate of export.

5. Conclusion

We set out to understand why phytoplankton concentrations are higher in anticyclonic eddies than in cyclonic eddies during the April to October period in an oligotrophic, nitrogen-limited, region off western Australia. As observations show that nitrate concentrations are depleted down to detection limit in the, up to 285 m deep, surface mixed layers of ACEs, this implies that the phytoplankton dynamics are predominantly controlled by the availability of nitrate rather than by other nutrients or light. Hence, we focussed on mechanisms supplying "fixed nitrogen" to the surface mixed layer of ACEs as a means to understand what is driving this anomalous behaviour.

From a suite of tracer release experiments in an eddy-resolving circulation model we disentangled the relative importance of "fixed nitrogen" supply from the shelf and, via diapycnal processes, from the nutrient-replete waters below the euphotic zone. Our experiments revealed that warm, low-salinity shelf water is predominantly exported into ACEs, which suppresses (diapycnal) entrainment associated with deepening surface mixed layers during austral autumn and winter. Correspondingly we find that the elevated phytoplankton concentrations in ACEs are driven predominantly by injection of shelf waters, which have relatively high concentrations of nitrate and particulate organic nitrogen, and to a lesser extent by diapycnal processes. In CEs the relative importance is the other way round. They receive less water from the shelf but receive more nutrients from the thermocline, starting in June–July

when their surface mixed layers deepen beyond the euphotic zone.

Although these results are essentially based on the ocean circulation model used, we have some confidence in these estimate since they are supported by the sparse observations available. First, both remote sensing and in situ observations support the importance of the shelf in initializing the ACEs with high phytoplankton and associated high particulate organic nitrogen concentrations. Further, in situ observations of the phytoplankton composition within ACEs are more akin to those found in shelf water than those found in offshore water surrounding the ACEs (Moore et al., 2007). Second, observed seasonal cycles of chlorophyll a with ACEs peaking in May–June and CEs later in August–September are consistent with the proposed nutrient supply pathways. Third, the "fixed nitrogen" supply estimated from the model simulations is consistent with observed changes of the "fixed nitrogen" content in ACEs and the only observation of particulate organic matter export we are aware of.

One outstanding question arising from our study is how the shelf off WA (here defined as bounded by the 200-m isobath) is replenished with nutrients. The "shelf water" tracer experiment proposed an export from the shelf to the open ocean of 1.8×10^{13} m^3 over the April–August period (corresponding to 1.7 Sv). Assuming a "fixed nitrogen" concentration on the shelf of 1.5 mmol N m^{-3} yields a corresponding loss of 27 Gmol "fixed nitrogen". Nitrogen fixation rates (Holl et al., 2007) on and river runoff (Moore, 2007) to the shelf are orders of magnitude smaller, which implies that an open ocean source of nutrients to the shelf must exist to balance the "fixed nitrogen" injected into the ACEs. Since our circulation model did not reveal any significant upwelling of thermocline waters high in nutrient content along the shelf break we speculate that the Leeuwin current might be a major source of "fixed nitrogen" to the shelf off WA.

Acknowledgements

References

Burchard, H., Rennau, H., 2008. Comparative quantification of physically and numerically induced mixing in ocean models. Ocean Modelling 20, 293–311.

Chen, D., Rothstein, L.M., Busalacchi, A.J., 1994. A hybrid vertical mixing scheme and its application to tropical ocean models. J. Phys. Oceanogr. 10, 2156–2179.

Dietze, H., Oschlies, A., Kähler, P., 2004. Internal-wave-induced and double-diffusive nutrient fluxes to the nutrient-consuming surface layer in the oligotrophic subtropical North Atlantic. Ocean Dyn. 54, 1–7.

Falkowski, P., Ziemann, D., Kolber, Z., Bienfang, P., 1991. Role of eddy pumping in enhancing primary production in the ocean. Nature 352, 55–58.

Feng, M., Meyer, G., Pearce, A., Wijffels, S., 2003. Annual and interannual variations of the Leeuwin current at 32°S. J. Geophys. Res. 108 (11), 3355.

Feng, M., Majewski, L.J., Fandry, C.B., Waite, A.M., 2007. Characteristics of two counter-rotating eddies in the Leeuwin current system off the western Australian coast. Deep-Sea Res. Part II 54, 961–980.

Greenwood, J.E., Feng, M., Waite, A.M., 2007. A one-dimensional simulation of biological production in two contrasting mesoscale eddies in the south eastern Indian ocean. Deep-Sea Res. Part II 54, 1029–1044.

Griffies, S., Gnanadesikan, A., Dixon, K., Dunne, J., Gerdes, R., Harrison, M., Rosati, A., Russell, J., Samuels, B., Spelman, M., Winton, M., Zhang, R., 2005. Formulation of an ocean model for global climate simulations. Ocean Sci. 1, 45–79.

Griffin, D., Wilkin, J., Chubb, C., Pearce, A., Caputi, N., 2001. Ocean currents and the larval phase of Australian western rock lobster, Panulirus cygnus. Mar. Freshwater Res. 52, 1187–1199.

Holl, C.M., Waite, A.M., Pesant, S., Thompson, P.A., Montoya, J.P., 2007. Unicellular diazotrophy as a source of nitrogen to Leeuwin current coastal eddies. Deep-Sea Res. Part II 54, 1045–1054.

Hundsorfer, W., Trompert, R., 1994. Method of lines and direct discretization—a comparison for linear advection. Appl. Numer. Math. 13, 469–490.

Jenkins, W., 1988. Nitrate flux into the euphotic zone near Bermuda. Nature 331, 521–523.

Lourey, M., Dunn, J., Waring, J., 2006. A mixed-layer nutrient climatology of Leeuwin current and western Australian shelf waters: seasonal nutrient dynamics and biomass. J. Mar. Syst. 59, 25–51

McGillicuddy, D., Robinson, A., 1997. Eddy-induced nutrient supply and new production in the Sargasso Sea. Deep-Sea Res. Part I 44, 1427–1450.

Moore, T., 2007. Physical oceanographic controls on phytoplankton distribution in the Banda sea and western Australian region. Ph.D. Thesis, University of Tasmania, Hobart, Australia.

Moore, T.S., Matear, R.J., Marra, J., Clementson, L., 2007. Phytoplankton variability off the western Australian coast: mesoscale eddies and their role in cross-shelf exchange. Deep-Sea Res. Part II 54, 943–960.

Oke, P.R., Schiller, A., Griffin, D.A., Brassington, G.B., 2005. Ensemble data assimilation for an eddy-resolving ocean model of the Australian region. Q. J. R. Meteorol. Soc. 131, 3301–3311.

Thompson, P., 1987. Continental-shelf-scale model of Leeuwin current. J. Mar. Res. 45, 813–827.

Tilburg, C., Subrahmanyam, B., O'Brien, J., 2002. Ocean color variability in the Tasman sea. Geophys. Res. Lett. 29.

Uppala, S., Kallberg, P., Simmons, A., Andrae, U., da Costa Bechtold, V., Fiorino, M., Gibson, J., Haseler, J., Hernandez, A., Kelly, G., Li, X., Onogi, K., Saarinen, S., Sokka, N., Allan, R., Andersson, E., Arpe, K., Balmaseda, M., Beljaars, A., van de Berg, L., Bidlot, J., Bormann, N., Caires, S., Chevallier, F., Dethof, A., Dragosavac, M., Fisher, M., Fuentes, M., Hagemann, S., Holm, E., Hoskins, B., Isaksen, L., Janssen, P., Jenne, R., McNally, A., Mahfouf, J.-F., Morcrette, J.-J., Rayner, N., Saunders, R., Simon, P., Sterl, A., Trenberth, K., Untch, A., Vasiljevic, D., Viterbo, P., Woollen, J., 2005. The era-40 re-analysis. Q. J. R. Meteorol. Soc. 131, 2961–3012.

Waite, A.M., Muhling, B.A., Holl, C.M., Beckley, L.E., Montoya, J.P., Strzelecki, J., Thompson, P.A., Pesant, S., 2007a. Food web structure in two counter-rotating eddies based on delta n-15 and delta c-13 isotopic analyses. Deep-Sea Res. Part II 54, 1055–1075.

Waite, A.M., Thompson, P.A., Pesan, S., Feng, M., Beckley, L.E., Domingues, C.M., Gaughan, D.J., Hanson, C.E., Holl, C.M., Koslow, K., Meuleners, M., Montoya, J.P., Moore, T.M., Muhling, B.A., Paterson, H., Rennie, S., Strzelecki, J., Twomey, L., 2007b. The Leeuwin current and its eddies: an introductory overview. Deep-Sea Res. Part II 54, 789–796.